EFFECTS OF BODYWEIGHT, HEIGHT, AND RIBCAGE AREA MOMENT OF INERTIA ON BLUNT CHEST IMPACT RESPONSE

Hideyuki Kimpara, Masami Iwamoto, Isao Watanabe and Kazuo Miki
TOYOTA Central R&D Labs., Inc.

Jong B. Lee, King H. Yang and Albert I. King
Bioengineering Center, Wayne State University

ABSTRACT

The purpose of this study was to determine the effects of bodyweight, height and ribcage area moment of inertia on human chest impact responses in frontal pendulum impacts. A series of parametric studies was conducted using a commercially available three-dimensional (3D) finite element (FE) model of the whole human body, Total HUman Model for Safety (THUMS). It was found that the maximum chest compression ratio, the best predictor of the number of rib fractures, was correlated with the area moment of inertia of the ribcage.

Keywords: Biomechanics, Thorax, Finite element method, Frontal impacts, Area moment of inertia

NORMALIZATION OR SCALING is a commonly used procedure to interpolate/extrapolate (normalize) impact response and tolerance data obtained from animals, volunteers, and/or cadavers of all sizes to the 5th, 50th, or 95th percentile human subject. Based on blunt chest impact data for male only subjects reported by Kroell et al. (1971), Neathery (1974) developed three separate sets of force-deflection corridors to represent the 5th, 50th and 95th percentile human using a scaling method based on Fourier's principle of dimensional homogeneity. Additionally, various scaling methods based on dimensional analysis have been proposed using the weight and/or height of the whole body (Eppinger et al. 1984, Mertz et al. 1989, Eppinger et al. 2000). Presently, little research has been done to investigate the effect of gender on the accuracy of scaling methods. A recent retrospective analysis of frontal chest pendulum impact, using data obtained by Nahum et al. (1970), Kroell et al. (1971 and 1974) and Stalnaker et al. (1972), found that the effect of gender was mainly from size differences instead of material properties (Kimpara et al. 2003). On the contrary, Kuppa et al. (2000) reported that gender has insignificant effect on injury outcomes.

In general, scaling methods assume that the human body can be represented by simple mechanical systems, such as the mass-spring-damper system reported by Lobdell et al. (1973). Therefore, the relationship between impact responses and the weight (or height) of the human body could be derived through dimensional analysis. Dimensional analysis has been used with success when predicting the weight and height of the human body and is being used for designing anthropomorphic test devices (ATDs) and computational models (Happee et al. 2000, Irwin et al. 2002, Kent et al. 2004, Mertz et al. 2003). However, the human body is too complex to be represented by a simple system. For example, the bony structure and material properties such as the density, stiffness, viscosity, etc. all contribute to the impact response of the chest region.

Mathematical models capable of predicting impact responses of the human body have been used to improve our understanding in the field of injury biomechanics. Many 3D FE human component models comprised of detailed anatomical features, such as those reported by Shah et al. (2001), Lee and Yang (2001), Iwamoto et al. (2002) and Kimpara et al. (2004a), have been developed to simulate impact responses, to reveal injury mechanisms, and to study the effect of varying biomechanical properties.

Validating the responses of a specific percentile subject may be difficult, mainly due to difficulties obtaining an adequate number of specimens in any specific size group. On the contrary, FE models have been shown to be an excellent tool when determining the effect of geometric and material properties. The aim of this study was to determine which of these parameters, namely the weight, height, and ribcage area moment of inertia, influenced impact responses of the chest in a

frontal pendulum impact through a parametric study using a commercially available finite element model. Findings obtained from this study would provide information needed for improving scaling methods applicable for the study of chest impact biomechanics.

METHODS

FE CHEST MODEL: A commercially available mid-sized human male model THUMS-AM50 (Version 1.52, Toyota Central R&D Lab., Inc.), reported by Iwamoto et al. (2002), was used as the baseline model to predict chest impact responses using the original geometric parameters of THUMS. This model was chosen because it had been validated against experimental data obtained from several impact scenarios, including impacts to the head, spine, shoulder complex, ribcage, pelvis, upper and lower extremities, and skin, using two explicit simulation codes: LS-DYNA (LSTC, Livermore, CA, USA) and PAM-CRASH (ESI, Paris, France). The basic anthropomorphic data of the THUMS-AM50 was based on data reported by Schneider et al. (1983) for a 50^{th} percentile adult human male. In order to reduce computational time, the length and width of typical elements were sufficiently large so that the initial minimum time step was greater than one microsecond.

The ribcage consists of the spine, sternum, costal cartilage, and 12 pairs of ribs composed of cortical and trabecular bones. In the baseline model, the ribs were modeled using one layer of shell elements and one layer of solid elements corresponding to cortical and trabecular bones, respectively. Nonlinear articulations of the ribcage, which included the sternocostal joints and the interchondral articulations, were treated as if they were directly connected similar to those reported by Wang (1995) and Lee and Yang (2001). However, costovertebral joints, the costotransverse joints between the ribs and vertebral body of the spine, were modeled as bone-to-bone contacts and the joint stiffness was controlled by major ligaments. All ligaments were modeled using tension-only elastic membrane or bar elements.

The model representing the 50^{th} percentile male (AM50) was considered to be the baseline model (Model 0). Geometrical details of the ribs reported in the literature were obtained mostly from the straight portion of the 6^{th} and 7^{th} ribs. Kimpara et al. (2004a) reported that the cross-sectional area and area moment of inertia for male cadaveric subjects were 29.6 ± 7.9 mm^2 and 209.6 ± 94.2 mm^4, respectively. Note that there are 12 pairs of ribs and the geometrical parameters for each rib are different. The average cross-sectional area and associated area moment of inertia used for the baseline model were 26.3 ± 1.8 mm^2 and 131.4 ± 32.0 mm^4, respectively.

Material properties used for the bones and soft tissues in the baseline model were based on published experimental data (Yamada 1970 and Abe et al. 1996) with minor modifications to fit model responses to experimental corridors. Stein and Granik (1976) and Kimpara et al. (2004b) reported that the human rib specimen behaved as an elastic-plastic material when loaded in three-point bending tests. On the other hand, Hayes (1991) found no plastic deformations when small pieces of cortical femur bone specimens were loaded under uniaxial tension or compression. In this study, elastic-plastic material characteristics were used so that rib fractures could be simulated using a mesh elimination method. The failure criteria assumed were 3% strain for cortical bone (LS-DYNA MAT Type 81 with element Type 16) and 10.3% for trabecular bone (LS-DYNA MAT Type 24 with element Type 1) of the rib cage, respectively.

It has been reported in the literature that cortical bone fails at a strain of around 2%. However, the threshold method used in LS-DYNA is very sensitive to the size of the mesh as well as material properties selected. After investigating the effect of different mesh size using either a 4-layer fine mesh or 1-layer coarse mesh model of the same geometry, it was determined that simulation results based on a failure strain of 3% matched better with experimental data when the current mesh density was employed. For trabecular bone, a failure strain of 10.3% was selected based on Hayes and Gerhart (1985) who reported that failure strains of the trabecular bone ranged from 3 to 23% before it was fully crushed with a significant increase in stiffness.

Internal organs in the chest cavity were modeled using a linear viscoelastic cellular rubber material with confined air pressure (LS-DYNA MAT Type 87) and internal organs in the abdominal cavity were modeled using a crushable foam material law (LS-DYNA MAT Type 63). The superficial muscles were modeled using a linear viscoelastic material and the skin was represented by linear elastic shell/membrane elements.

Table 1 – Material properties for the cortical bones used in this study

	Mass density	Young's modulus	Yield stress	Shell thickness
	(kg/m^3)	(GPa)	(MPa)	(mm)
Rib's cortical bone	2,000	10.2	65.3	0.7
Sternum's cortical bone	2,000	11.5	123.0	1.0

SIMULATION MATRIX: Three body sizes: a large male (AM95) with a weight of 102.6 kg and a height of 186.4 cm, a mid-size male (AM50) with a weight of 76.6 kg and a height of 175.1 cm, and a small female (AF05) with a weight of 46.4 kg and a height of 151.1 cm were simulated. To obtain the scale factor based on an equal-stress equal-velocity procedure proposed by Eppinger et al. (1984), the body weight ratio λ_m was calculated first. Based on the weight ratio, the scaling factor for AM95 and AF05 was 134% and 60.6%, respectively. The length dimensions, such as the height, chest depth and the thickness of the cortical bones, ligaments, skin and other tissues were scaled from λ_m using the cubic root ($\lambda_m^{1/3}$). Based on these two λ_m values, the corresponding cubic roots for AM95 and AF05 was 110.25% and 84.63% for $\lambda_m^{1/3}{}_{AM95}$ and $\lambda_m^{1/3}{}_{AF05}$, respectively. For simplicity, the length scaling factors for $\lambda_m^{1/3}{}_{AM95}$ and $\lambda_m^{1/3}{}_{AF05}$ used were 110% and 85%, respectively.

A total of 11 simulation models, including the baseline Model 0, were prepared for frontal pendulum impact simulations (Table 2). These models represent several variations in human anthropometry, as explained in detail below. In Model 1, all length dimensions, such as the rib thickness, ligament length and vertebral body height, were enlarged by 110% to represent a large male while in Model 2, all length dimensions were reduced to 85% to represent a small female. Note that the mass density for Models 1 and 2 did not need to be changed to reflect the proper weight. Figure 1 shows the features of the baseline model (Model 0), large male model (Model 1), and small female model (Model 2).

Table 2 – Simulation matrix

	Human body		Area Moment of Inertia	
	Weight	Height	Sternum	Ribs
Model 0	AM50	AM50	AM50	AM50
Model 1	AM95	AM95	AM95	AM95
Model 2	AF05	AF05	AF05	AF05
Model 3	AM95	AM50	AM50	AM50
Model 4	AF05	AM50	AM50	AM50
Model 5	AM50	AM95	AM95	AM95
Model 6	AM50	AF05	AF05	AF05
Model 7	AM50	AM50	AM95	AM95
Model 8	AM50	AM50	AF05	AF05
Model 9	AM50	AM50	AM50	AM95
Model 10	AM50	AM50	AM50	AF05

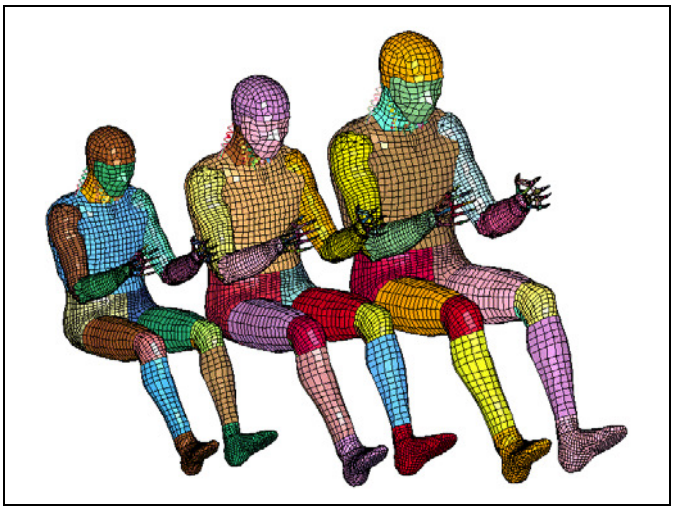

Figure 1 – FE Human models (from left): small female model (Model 2), baseline male model (Model 0) and large male model (Model 1)

Models 3 and 4 represented a person with all length dimensions the same as those for an AM50 but with either the weight of either an AM95 or AF05. To achieve these goals, the mass density was multiplied by either 134% or 60.6% of the baseline model. In Model 5, a tall and skinny person (with the height and cross-sectional properties of an AM95 and the same weight as an AM50) was simulated. To achieve this goal, all length dimensions of the baseline model were multiplied by 110% while the mass density was multiplied by 75.1% (inverse of $\lambda_{m\ AM95}$) so that the total mass remained the same as that for an AM50. In Model 6, a short but heavy person (with the height and cross-sectional properties of an AF05 and the same weight as an AM50) was simulated.

Models 7 through 10 were created to simulate persons with irregular proportion of cross-sectional area compared to the baseline model. Model 7 represented the size of an AM50, but the area moment of inertia for the ribcage (ribs and sternum) was increased to the same size as that used in an AM95. In contrast, Model 8 represented the size of an AM50 but the area moment of inertia for the ribcage (ribs and sternum) was the same as an AF05. To achieve these goals of increasing or decreasing the moment of inertia without changing the dimensions of the ribcage, an increase of 44.3% and a decrease of 47.2% in the cortical bone thickness of the ribs and sternum were implemented (Figure 2). For Model 7, the cortical bone thickness was increased from 0.70 to 1.01 mm and 1.00 to 1.44 mm for the rib and sternum, respectively. Similarly, the cortical thickness for Model 8 was changed from 0.70 to 0.37 mm and 1.00 to 0.53 mm for the rib and sternum, respectively. Models 9 and 10 assumed that the area moment of inertia for the rib was the same as that used in Models 7 and 8, respectively. However, the area moment of inertia of the sternum was the same as an AM50.

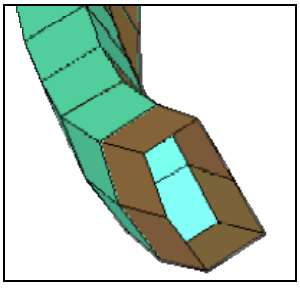

Figure 2 – Structure of the rib model: rib model has shell and solid elements that represent cortical and trabecular bone respectively.

SIMULATION SETUP: All 11 models were positioned to duplicate the pendulum impact tests reported by Kroell et al. (1971 and 1974) for frontal impact (Figure 3). The model was positioned in an erect sitting position on a rigid flat surface with a free-back boundary condition because the

purpose of this study was to investigate the effect of the body weight and height on frontal pendulum impact chest impact responses, including the inertia of the torso. Kroell et al. (1974) reported that the fixed-back test configuration precluded whole body motion, and provides no information regarding the effect of body weight and height. Consequently, only the free-back test configuration was selected for this study. The impact was directed to the mid-sternum at an initial velocity of 6.9 m/s. The pendulum had a mass of 23.4 kg and a diameter of 150 mm with the impacting edge rounded. Impact force and chest deflection were calculated using a commercially available FE solver, LS-DYNA 970 revision 5434 (LSTC, Livermore, CA) using an Intel based computer running a Red-Hat Linux 7.3 operating system. Post-processing of simulation results was conducted using the LS-PREPOST post-processing program (LSTC, Livermore, CA.). Results predicted by the model were sampled at 10 kHz and contact force data were filtered using an SAE digital low pass filter at a channel frequency class (CFC) of 1,000 Hz.

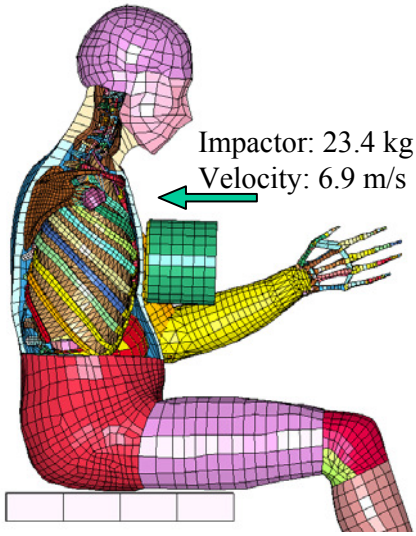

Figure 3 – Simulation setup of the THUMS model for frontal pendulum chest impact

LINEAR REGRESSION ANALYSIS: A linear regression analysis was conducted to evaluate the effect of variances in anthropometrics and to find the optimal injury predictor. Commercially available software, STATISTICA (StatSoft, Inc., Tulsa, OK), was used for analysis.

RESULTS

MODEL VALIDATION: Figure 4 shows the force-deflection response predicted by the baseline model (Model 0) and corridors drawn based on the average and plus/minus one standard deviation calculated from Test Number 13FM, 15FM, 18FM, 19FM, 20FM, 22FM and 64FM reported by Kroell et al. (1971, 1974) for frontal pendulum impact. The initial chest stiffness (K), maximum chest force (F_{max}), maximum chest deflection (D_{max}), and maximum chest compression ratio (C_{max}) were calculated from the force-deflection curve predicted by the model. Additionally, the number of rib fractures (Rib Fxs) and the number of fractured ribs (Fxed Ribs) predicted by the model were used to correlate with experimentally obtained rib fractures. However, the viscous criteria (VC and V) could not be recreated from the papers selected for this study because the viscous criterion reported by Viano et al. was not available until 1989. The K was calculated from the initial linear portion of the force-deflection curve for correlation with model input parameters (Figure 4). The baseline model (Model 0) predicted 14 rib fractures on nine ribs, a maximum chest deflection of 88.1 mm, a maximum contact force of 4.5 kN, a maximum compression ratio of 37.3%, and an initial chest stiffness of 431 kN/m. The predicted force-deflection response was validated against the corridor of the experimental data. A significant drop in the impact force after the initial force peak was believed to be a common phenomenon associated with impacting a viscoelastic structure. Several of experimental test results reported by Kroell et al. (1971 and 1974) also exhibited a similar drop of 30% or more.

Additionally, model predicted number of rib fractures was reasonable compared to 10.1 ± 8.3

fractures obtained from Test Number 13FM, 15FM, 18FM, 19FM, 20FM, 22FM and 64FM (Kroell et al. 1971 and 1974). The number of rib fractures was counted by the number of shell elements eliminated while the number of fractured ribs was determined by the number of rib which has shell elements eliminated. Circles in Figure 5 mark the locations of model predicted rib fractures. In Figure 6, the time at which a rib fracture occurred is denoted. Figure 7 shows the force-deflection response curves for all simulations. Table 3 lists all response variables for all simulations. In this table, numbers shown in parentheses mean the percentage change based on values predicted for the baseline model. Shaded cells in Table 3 represents those cases with a decrease in the impact response for the sake of differentiate those with an increase and a decrease in model predicted responses.

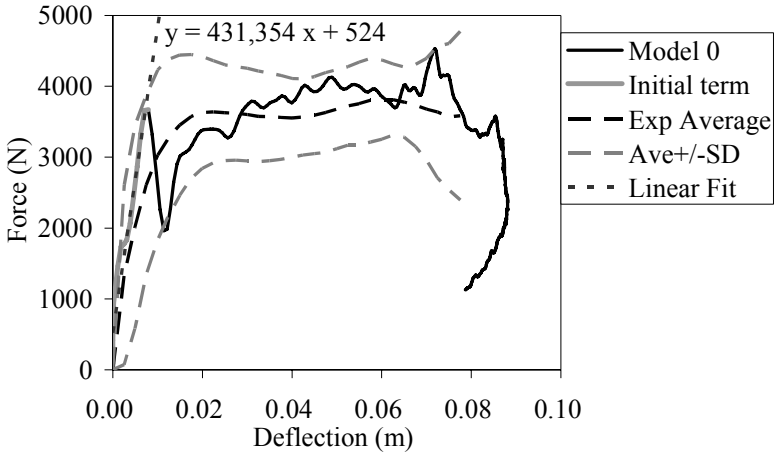

Figure 4 – Comparison of the force-deflection responses with the corridors generated from cadaveric data obtained by Kroell et al. (1971 and 1974)

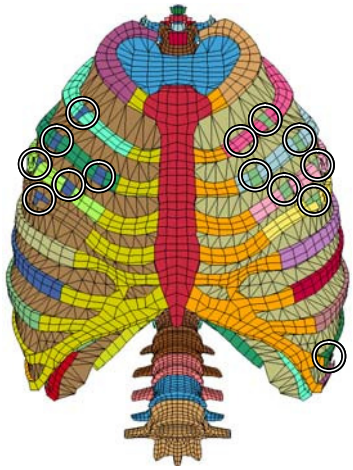

Figure 5 – Rib fracture locations predicted by the baseline model (Model 0) at t=45 ms

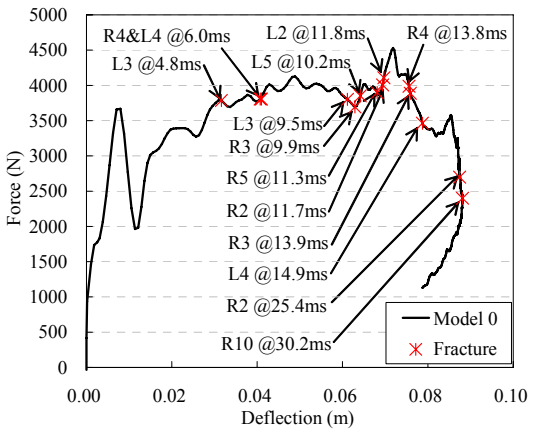

Figure 6 – Relationship between the overall chest deflection and rib fracture for the baseline model (Model 0)

Table 3 – Summary of the stiffness, peak force, maximum chest deflection, maximum compression ratio, number of rib fractures, and number of fractured ribs for each simulation case. Shaded cells indicate a decrease in model predicted responses

	K [kN/m]	F_{max} [kN]	D_{max} [mm]	C_{max} [ ]	Rib Fxs*[1]	Fxed Ribs*[2]
Model 0	431	4.5	88.1	37.3	14	9
Model 1	**563 (+30.4%)**	**4.7 (+3.5%)**	**93.1 (+5.7%)**	35.8 (-4.0%)	11 (-3)	8 (-1)
Model 2	**465 (+7.8%)**	4.2 (-7.7%)	76.3 (-13.4%)	**38.0 (+1.9%)**	**15 (+1)**	**11 (+2)**
Model 3	**558 (+29.3%)**	**4.8 (+6.5%)**	86.1 (-2.3%)	36.4 (-2.3%)	**16 (+2)**	9 (0)
Model 4	294 (-31.9%)	3.9 (-14.8%)	84.8 (-3.7%)	35.9 (-3.7%)	11 (-3)	8 (-1)
Model 5	**476 (+10.4%)**	4.2 (-7.6%)	**93.1 (+5.7%)**	35.8 (-3.9%)	11 (-3)	8 (-1)
Model 6	**627 (+45.2%)**	**4.9 (+8.0%)**	80.3 (-8.8%)	**40.0 (+7.3%)**	**25 (+11)**	**19 (+10)**
Model 7	**445 (+3.1%)**	**4.6 (+1.5%)**	84.9 (-3.7%)	35.9 (-3.7%)	12 (-2)	9 (0)
Model 8	417 (-3.3%)	4.1 (-8.8%)	**92.2 (+4.6%)**	**39.0 (+4.6%)**	**23 (+9)**	**16 (+7)**
Model 9	**432 (+0.2%)**	**4.6 (+1.8%)**	86.6 (-1.7%)	36.6 (-1.7%)	13 (-1)	**10 (+1)**
Model 10	430 (-0.2%)	4.1 (-10.5%)	**89.9 (+2.0%)**	**38.0 (+2.0%)**	**21 (+7)**	**15 (+6)**

*[1] Rib Fxs: number of rib fractures, *[2] Fxed Ribs: number of fractured ribs

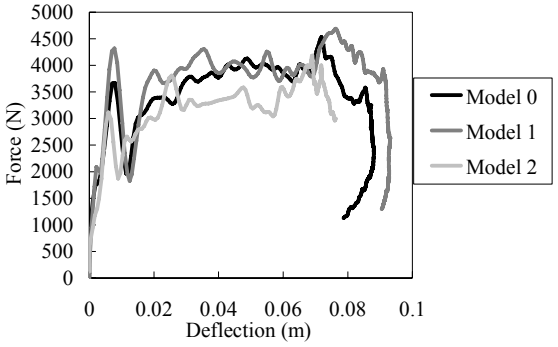

(a) Models 0, 1 and 2

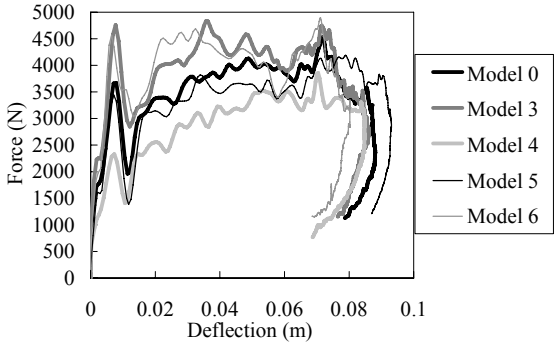

(b) Models 0, 3, 4, 5 and 6

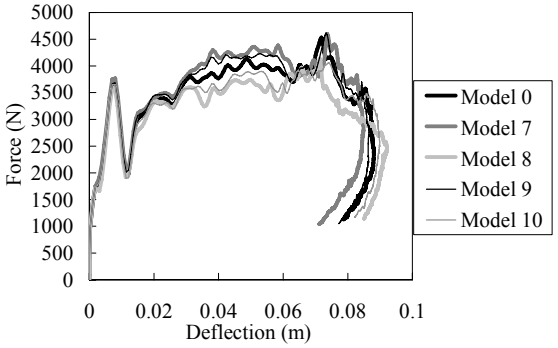

(c) Models 0, 7, 8, 9 and 10

Figure 7 – Comparison of force-deflection responses predicted by each simulation case compared to that predicted by the baseline model

LINEAR REGRESSION: Linear regressions were conducted among response variables (K, F_{max}, D_{max} and C_{max}) and predictor variables (bodyweight, height, and area moment of inertia of the ribcage and ribs alone). Bold face in Tables 4 and 5 indicates that the correlation was statistically significant. Table 4 lists the correlation coefficient (r^2) and significance level (p) with bold face values indicating statistical significance. It can be seen that K ($r^2 = 0.41$ and $p = 0.03$) and F_{max} ($r^2 = 0.45$ and $p = 0.02$) are poorly correlated with bodyweight, while D_{max} ($r^2 = 0.81$ and $p < 0.001$) is highly correlated with height, and C_{max} ($r^2 = 0.51$ and $p = 0.01$) is poorly correlated with height. Additionally, C_{max} is highly correlated with the area moment of inertia of the ribcage ($r^2 = 0.74$ and $p = 0.001$) and the area moment of inertia of the ribs alone ($r^2 = 0.73$ and $p = 0.001$). The model predicted number of rib fractures and fracture ribs was also linearly correlated with chest impact responses K, F_{max}, D_{max} and C_{max} (Table 5). It can be seen that C_{max} is highly correlated with the number of the rib fractures ($r^2 = 0.87$ and $p < 0.001$) and the number of fractured ribs ($r^2 = 0.89$ and $p < 0.001$) while K, F_{max} and D_{max} did not correlate with these two variables.

Table 4 – Linear correlation of the chest impact responses with the bodyweight, height, and area moment of inertia of the ribcage and ribs alone

	K		F_{max}		D_{max}		C_{max}	
	r^2	p	r^2	p	r^2	p	r^2	p
Weight	**0.41**	**0.03**	**0.45**	**0.02**	0.31	0.08	0.027	0.63
Height	0.034	0.59	0.016	0.71	**0.81**	**0.000**	**0.51**	**0.01**
Area moment of inertia of the ribcage	0.0020	0.90	0.013	0.74	0.30	0.08	**0.74**	**0.001**
Area moment of inertia of the ribs alone	0.0011	0.92	0.073	0.42	0.16	0.22	**0.73**	**0.001**

Table 5 – Cross reference of the rib fractures by the chest impact responses

	Rib Fxs		Fxed Ribs	
	r^2	p	r^2	p
K	0.11	0.31	0.096	0.35
F_{max}	0.093	0.78	0.070	0.84
D_{max}	0.024	0.65	0.043	0.54
C_{max}	**0.87**	**$p < 0.001$**	**0.89**	**$p < 0.001$**

DISCUSSION

INITIAL STIFFNESS (K) AND MAXIMUM CONTACT FORCE (F_{max}): We have used 11 numerical models to determine the effect of bodyweight, height, and area moment of inertia of the ribcage (ribs and sternum) and ribs alone on model predicted initial stiffness (K) and maximum contact force (F_{max}). Linear regression indicated that bodyweight, an inertial parameter, can only explain some of the observed changes in K ($r^2 = 0.41$) and F_{max} ($r^2 = 0.45$). Although statistically significant, the bodyweight can only explain part of the initial stiffness and the maximum contact force. Another reason is the fact that different tissues were exposed to the pendulum when different model sizes were simulated. Figure 8 shows the contact area imposed by the pendulum on the chest wall for the three body sizes (AM95, AM50, and AF05). The sternum, costal cartilage and ribs in Figure 8 were represented in dark, white and gray colors, respectively. As can be seen in this figure, the entire sternum was in contact with the pendulum for AF05 while only a portion of the sternum was impacted in AM95. Changes in the height and area moment of inertia of the ribcage and ribs alone were not correlated with K and F_{max}.

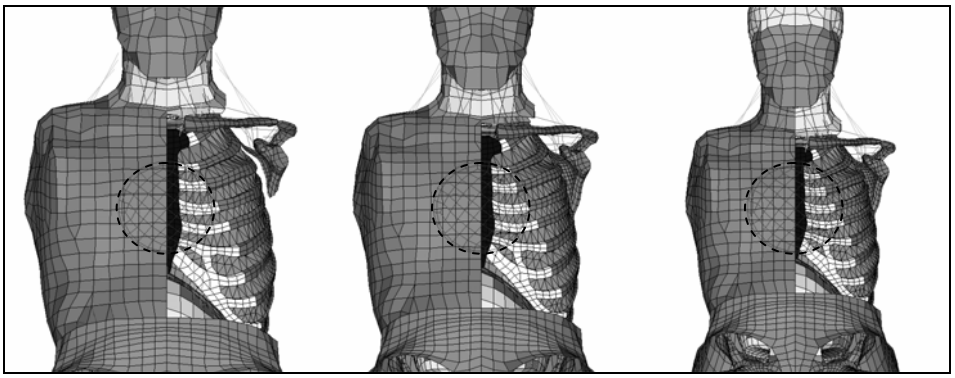

Figure 8 – Contact area of the pendulum on the chest for different body sizes (left: large male AM95, center: mid-size male AM50, right: small female AF05)

MAXIMUM CHEST DEFLECTION (D_{max}) AND COMPRESSION RATIO (C_{max}): Table 4 shows that D_{max} is significantly correlated with height ($r^2 = 0.81$) while C_{max} is poorly correlated with the height ($r^2 = 0.51$). C_{max} is highly correlated with area moment of inertia of the ribcage ($r^2 = 0.74$), and ribs alone ($r^2 = 0.73$). The finding of a linear relationship between D_{max} and height agrees in part with the scaling method proposed by Eppinger et al. (2000) which stated that an increase in size results in an increase in the chest deflection. On the other hand, results from this study show that C_{max}, which is calculated by dividing D_{max} by the initial chest depth, was more significantly affected by the area moment of inertia of the ribcage. The scaling method proposed by Eppinger et al. (2000) assumed that the maximum compression ratio should remain constant for different body sizes using the equal-stress equal-velocity scaling procedure. In contrast, our results showed that the height and cross-sectional properties of the ribcage both affect the maximum compression ratio. Additionally, the area moment of inertia of the ribcage (rib and sternum) and the area moment of inertia of the ribs alone are better predictors when calculating C_{max}. At present, the area moment of inertia of the ribs was not routinely reported by the impact biomechanics community. Consequently, geometric properties of the rib were not available in whole body impact tests. It is recommended that future whole body tests should include measurements of rib area moment of inertia as an anthropometric parameter in order to normalize the biomechanical responses and tolerances of the human body.

RIB FRACTURES: The location and number of rib fractures were predicted using the element elimination method available in LS-DYNA. No statistical significance was observed between the model predicted number of rib fractures and fractured ribs and global response variables K, F_{max}, and D_{max} (Table 5). On the other hand, C_{max} is capable of predicting the number of rib fractures and fractured ribs accurately with a r^2 value of 0.87 and 0.89, respectively. In cadaveric studies, the Abbreviated Injury Scale (AIS) for the chest injury severity was derived from the number of fractured ribs. Consequently, results from this study suggest that the maximum chest compression ratio would be a better predictor when estimating the risk of chest injury.

LIMITATIONS AND FUTURE WORK: Because cadaveric specimens of a specific size are very difficult to obtain for impact tests, only the baseline 3D human model was validated against 50th percentile human cadaveric data. The baseline model was scaled to represent different height and weight combination, without validation, to determine the effect of various biomechanical parameters on overall impact responses. Future studies need to address validation of these model variations. This study provides some critical data which explain the effect of bodyweight, height, and area moment of inertia of the ribcage on K, D_{max}, F_{max}, and C_{max} to better understand blunt impact response of the chest. However, the study considered only frontal pendulum impacts without belted or distributed loading conditions, assumed no gender differences in terms of material properties, and did not consider other response variables such as TTI or V*C. Therefore, further studies using cadavers tested in other loading conditions are needed to improve our understanding of the chest injury biomechanics.

Since only the baseline male model (AM50) was validated, results and conclusions drawn from this study could be improved by validating the 5th and 95th percentile models. To achieve this goal, it would be necessary to obtain experimental corridors for these two groups. Because the LS-DYNA code is very sensitive to mesh size and cortical bone failure strain was assumed at 150% of the reported experimental value, confidence in the results can be improved by performing sensitivity analyses. Similarly, the assumed trabecular bone failure strain of 10.3% was arbitrarily chosen, it is necessary to perform sensitivity analyses on this parameter by varying strains from 3 to 23% (see Methods) found in experimental studies. Additionally, it may be necessary to refine the models with more accurate moment of inertia as the current model used a value of 131.4 cm^2 which is somewhat lower than the experimentally obtained value of 209.6 cm^2 (Kimpara et al, 2004a). These refinements will add to the confidence in the results and conclusions of the present study.

CONCLUSIONS

The following conclusions are drawn from this study, based on 11 numerical simulations of frontal pendulum impacts using models scaled from the AM50 THUMS model:

1. Initial chest stiffness poorly correlates with bodyweight.
2. Maximum chest deflection is significantly correlated with height.
3. Maximum chest compression ratio correlated significantly with the area moment of inertia of the ribcage and of the ribs.

References

1) Abe, H., Hayashi, K., Sato, M. (Eds.), (1996): Data Book on Mechanical Properties of Living Cells, Tissues, and Organs, Springer
2) Association for the Advancement of Automotive Medicine (AAAM), (1990): The abbreviated injury scale 1990 revision, Des Plaines, IL
3) Eppinger, R.H., Marcus, J.H. and Morgan, R.M., (1984): Development of dummy and injury index for NHTSA's thoracic side impact protection research program, SAE 840885, Society of Automotive Engineers, Warrendale, PA
4) Eppinger, R., Sun, E., Kuppa, S., and Saul, R., (2000): Supplement: Development of Improved Injury Criteria for the Assessment of Advanced Automotive Restraint Systems – II, National Highway Traffic Safety Administration, U.S. Department of Transportation, Washington, D.C.
5) Happee, R., Ridella, S., Nayef, A., Morsink, P., de Lange, R., Bours, R. and van Hoof, J., (2000): Mathematical human body models representing a mid size male and a small female for frontal, lateral and rearward impact loading, Proc. of 2000 International Research Council on the Biomechanics of Impact (IRCOBI), pp. 67-81, Montpellier (French)
6) Hayes, W.C., and Gerhart, T.N., (1985): Biomechanics of bone: Applications for assessment of bone strength. In: Bone and Mineral Research, edited by Peck, W.A., pp. 259-294, Elsevier Science Publishers, Amsterdam
7) Hayes, W.C., (1991): Biomechanics of cortical and trabecular bone: implications for assessment of fracture risk, ed. Mow, V.C. and Hayes, W.C., Basic Orthopaedic Biomechanics, Raven Press. Ltd., New York, pp.93-142
8) Irwin, A.L., Mertz, H.J., Elhagediab, A.M. and Moss S., (2002): Guidelines for assessing the biofidelity of side impact dummies of various sizes and ages, Stapp Car Crash Journal, Vol.46, 2002-22-0016, pp.297–319
9) Iwamoto, M., Kisanuki, Y., Watanabe, I., Furusu, K., Miki, K. and Hasegawa, J., (2002): Development of a finite element model of the total human model for safety (THUMS) and application to injury reconstruction, Proc. of 2002 IRCOBI Conference, pp. 31-42, Munich.
10) Kent, R., Bass, C.R., Woods, W., Sherwood, C., Madeley, N.J., Salzar, R. and Kitagawa, Y., (2003): Muscle Tetanus and Loading Condition Effects on the Elastic and Viscous Characteristics of the Thorax, Traffic Injury Prevention, vol. 4, pp.1–18,
11) Kimpara, H., Iwamoto, M., Miki, K., Lee, J.B., Begeman, P.C., Yang, K.H. and King, A.I., (2003): Biomechanical properties of the male and female chest subjected to frontal and lateral impacts, Proc. of 2003 International Research Council on the Biomechanics of Impact (IRCOBI), Lisbon

(Portugal)
12) Kimpara, H., Iwamoto, M., Watanabe, I., Miki, K., Lee, J.B., Yang, K.H. and King, A.I., (2004a): Effects of strain rate and gender on properties of human ribs, 5th Combined Meeting of the Orthopaedic Research Societies of Canada, USA, Japan, and Europe, October 2004, Banff, Canada.
13) Kimpara, H., Iwamoto, M., Watanabe, I., Miki, K., Lee, J.B., Yang, K.H. and King, A.I., (2004b): Numerical analysis of the biomechanical characteristics and impact response of the human chest, 2004 ASME International Mechanical Engineering Congress and RD&D EXPO, November 2004, Anaheim, CA.
14) Kroell, C.K., Schneider, D.C. and Nahum, A.M., (1971): Impact Tolerance and Response of the Human Thorax, Proc. of the 15th Stapp Car Crash Conference, SAE Paper No. 710851
15) Kroell, C.K., Schneider, D.C. and Nahum, A.M., (1974): Impact Tolerance and Response of the Human Thorax II, Proc. of the 18th Stapp Car Crash Conference, SAE Paper No. 741187.
16) Kuppa, S., Eppinger, R., Maltese, M., Naik, R., Yoganandan, N., Pintar, F., Saul, R., McFadden, J., (2000): Assessment of thoracic injury criteria for side impact, IRCOBI 2000 pp. 131-146.
17) Lee, J. B. and Yang, K. H., (2001): Development of a finite element model of the human abdomen, Stapp Car Crash Journal, Vol.45, 2001-22-0004
18) Lobdell, T. E.; Kroell, C. K.; Schneider, D. C.; Hering, W. E. and Nahum, A. M. (1973): Impact Response of the Human Thorax, Human Impact Response Measurement and Simulation, W.F. King, H.J. Mertz, eds., Plenum Press, London, pp.201-45.
19) Mertz, H.J., Irwin, A.L., Melvin, J.W., Stalnaker R.L. and Beebe, M.S., (1989): Size, weight and biomechanical impact response requirements for adult size small female and large male dummies, SAE 890756, Society of Automotive Engineers, Warrendale, PA
20) Mertz, H.J., Irwin, A.L. and Prasad, P., (2003): Biomechanical and scaling bases for frontal and side impact injury assessment reference values, Stapp Car Crash Journal, Vol. 47, pp. 155-188
21) Nahum, A.M., Gadd, C.W., Schneider, D.C. and Kroell C.K., (1970): Deflection of the human thorax under sternal impact, SAE 700400, Society of Automotive Engineers, Warrendale, PA
22) Neathery, R.F., (1974): Analysis of chest impact response data and scaled performance recommendations, Proc. of the 18th Stapp Car Crash Conference, SAE Paper No. 741188
23) Schneider, L.W., Robbins, D.H., Pflug, M.A. and Snyder, R.G., (1983): Anthropometry of Motor Vehicle Occupants, Vol. 2,
24) Shah, C.S., Yang, K.H., Hardy, W., Wang, H.K. and King A.I., (2001): Development of a computer model to predict aortic rupture due to impact loading, Stapp Car Crash Journal, Vol.45, 2001-22-0007
25) Stalnaker, R.L., McElhaney, J.H., Roberts, V.L. and Trollope, M.L., (1972): Human torso response to blunt trauma, ed. King, W.F. and Mertz H.J., Human impact response, Proc. of the Symposium on Human Impact Response, New York, Plenum Press, pp.181-199, 1973
26) Stein, I.D. and Granik, G., (1976): Rib structure and bending strength: an autopsy study, Calcified tissue research, Vol. 20, pp.61-73
27) Wang, H.-C. K. (1995): Development of a Side Impact Finite Element Human Thoracic Model, Ph. D. dissertation, Wayne State University, Detroit, Michigan.
28) Yamada, H., (1970): Strength of Biological Materials, Williams & Wilkins Company